Electron-impact ionization of atomic hydrogen at intermediate energies

Jamal Berakdar*
Atomic and Molecular Physics Laboratories, Research School of Physical Sciences and Engineering, Australian National University, Canberra, ACT 0200, Australia
(Received 15 January 1997)

The electron-impact ionization of atomic hydrogen at intermediate excess energies is considered in the situation where the two continuum electrons escape with substantially different velocities and coplanar with the incident direction. Calculations are performed within a model where the three-body final state is described by a product wave function consisting of three symmetrical, Coulomb-type functions. Each of these functions describes the motion of a particular two-body subsystem in the presence of the third charged particle. A comprehensive comparison with available experimental data is presented, and the results are contrasted with those of other theoretical models. Generally, good agreement is found with the absolute measurements; however, in some cases discrepancies between various theoretical predictions and experimental findings are obvious, which highlights the need for a theoretical and experimental benchmark study of these reactions. [S1050-2947(97)07106-0]

PACS number(s): 34.80.Dp

The first experimental studies on electron-impact ionization of atomic systems with fully determined kinematics of the reaction fragments [hereafter called $(e,2e)$] were conducted at moderate incident energies (a few times the ionization potential) with little momentum being transferred to the target [1–5]. Under these conditions two continuum electrons emerge with substantially different energies, and are detected coplanar with the incident direction. This geometry is an ideal candidate for benchmark measurements since, in this case, the magnitude of the cross section is particularly large, and the small momentum transferred to the target allows an extrapolation to known absolute photoionization cross sections [4]. Such measurements, in particular for the ionization of atomic hydrogen which leads to a pure three-body final state, are of prime importance in assessing theoretical approaches to the nonseparable, three-particle Coulomb continuum problem. For the ionization of atomic hydrogen in the ground state, the measured angular distribution of the slow secondary electron exhibits a double-peak structure whose positions are mainly associated with the direction of the momentum-transfer vector $\hat{\mathbf{q}}$. A dominant peak appears roughly around the direction $\hat{\mathbf{q}}$ and can be assigned to a direct (classical) projectile-electron encounter. Hence, this peak is called the *binary* peak [4,6,7]. A further, less pronounced peak, the *recoil peak*, is situated around $-\hat{\mathbf{q}}$ and can be interpreted as the result of a sequential scattering process in which the target electron recoils off the nucleus after a direct scattering from the projectile [8]. The recoil scattering from the nucleus can occur via initial-state binding. The above-mentioned mechanisms for the emergence of the binary-recoil peak structure are qualitatively present even in the simplest theoretical treatment in which plane waves for incoming and outgoing particles are assumed [8]. In contrast, a quantitative theoretical description of the experimental findings, in particular the absolute magnitude of the cross section, turned out to be an intriguing task. Perturbative approaches using the Born series (whose convergence properties are unclear for reactions involving infinite-range Coulomb potentials) seem to reproduce quantitatively some features of the measured angular distributions [6,9,10]. However, the range of validity of such approaches is difficult to estimate. Another approach using the (square integrable) pseudostate close-coupling method (PSCC) [11,12] resulted in generally good, although not perfect, agreement with the experimental data. A recent convergent close-coupling study (hereafter CCC) [13] employs an orthogonal Laguerre basis to diagonalize the target Hamiltonian. Convergence is checked with respect to the basis size. In the final state the two electrons are treated asymmetrically, one occupying a plane wave whereas a Coulomb wave is assumed for the other electron. As stated in Ref. [13], for the case of hydrogenic targets this numerical approach treats the scattering problem essentially without approximation. Nonetheless, some discrepancies between the CCC results and the experimental findings are observed [13] (comparison is included below). In addition, the CCC method predicts additional subsidiary structures in the angular distributions whose origins are yet to be explained.

In an analytical treatment of this process, one focuses on the three-body final state (two electrons in the residual ion field), and attempts to derive approximate expressions for this state. An approximation, which has previously been proposed for ion-atom collisions [14], was adopted to $(e,2e)$ reactions with remarkable success [15,16], as far as the relative angular distributions are concerned. In this approximation individual (isolated) two-body scatterings are treated to infinite order (in a perturbative sense), which is the origin of the correct asymptotic behavior at large interparticle separations. This wave function is called 3C hereafter, as it consists of three Coulomb waves (the interelectronic plane-wave part being omitted) each simulating an isolated two-body scattering. The success of the 3C approach in describing the rela-

*Present address: Max-Planck-Institute for Microstructure Physics, Weinberg 2, 06120 Halle, Germany. Electronic address: jber@mpi-Halle.mpg.de

tive shape of the measured experimental data triggered a continuing debate about the importance of boundary conditions [15–21]. An interelectronic Coulomb phase factor was added to the distorted-wave Born approximation (3DWBA) in order to restore the boundary condition at large interparticle separations [20]. In Ref. [17] the first Born approximation has been modified by two Coulomb phase factors to result in a correct asymptotic behavior. Although these modifications have led to significant improvements (as far as agreement with experiment is concerned) the effect of the high oscillatory behavior of these phase factors at lower energies is not clear. Further investigations of the asymptotic properties of the three-body Schrödinger equation showed that a proper description of the asymptotic regime, where two particles approach each other while far away from the third one, requires the introduction of local relative momenta [22] (this treatment is hereafter called the AM model). No attempt at describing the short-range dynamics has been undertaken. Application of the derived wave function to the present reaction is hampered by two major obstacles which are typical for sophisticated analytical (beyond 3C) models. Due to the complicated analytical form of the wave function, scattering amplitudes have to be deduced numerically. This necessitates a six-dimensional numerical integration. Of particular difficulty is the long-range integration over the projectile coordinates. This problem was recently attacked [21,23–25]. These kinds of numerical studies will shed new light on the importance of the inclusion of proper boundary conditions since they offer a direct insight into the contributions of various regimes of the phase space to the scattering amplitudes. The second difficulty associated with the AM wave function is the evaluation of its normalization. An expression for this normalization was proposed in Ref. [22]; however, no justifications for this particular choice were given. One might think of deducing the normalization by requiring that the asymptotic flux generated by such functions must be identical to that associated with plane waves. While imposing this requirement improves the asymptotic flux properties of the wave functions used, it does not yield the correct normalization as derived from a six-dimensional integration over the configuration space. For example, a singular short-range behavior of a wave function would not affect the asymptotic flux, and hence its flux normalization, but would certainly show up in an integration over the entire configuration space. As this ''approximate'' normalization severely influences the angular distributions, calculations with the AM wave function, as proposed in Ref. [22], do not provide unique information on the range of validity of the approximations assumed in the Schrödinger equation to arrive at the radial part of the wave function.

These same two difficulties are encountered in a further treatment which deals with the short-range dynamics by incorporating some rotationally invariant properties of the total potential surface into the wave function [26] while maintaining a proper asymptotic. This approach and its subsets, as well as the methods employed to deal with the aforementioned problems, are briefly discussed in Sec. I. Low-energy measurements were reasonably reproduced and interpreted by this method. In this work application is extended to intermediate energies with small momentum transfer. Although the prediction of this model can be considered satisfactory, in some cases there are still substantial differences between theoretical predictions (including those from other theories) and experiment. Thus further theoretical and experimental work is required in order to establish benchmark data for this most fundamental case of $(e,2e)$ processes. Throughout this work atomic units are used. Corrections due to a finite electron-proton mass ratio are neglected.

I. THEORETICAL APPROACH

The 3C approach is a nonperturbative method which treats all two-body interactions on equal footing. However, it does not account for coupling between each of the two-body subsystems to the third particles; i.e., within the 3C model the charged particles move due to their mutual two-body potential, which is quite different from the total potential. For example, the electron-electron scattering is considered as an isolated two-body Rutherford scattering, whereas, according to Wannier analysis [27–36], which is based on properties of the *total* potential, one obtains a free motion of the two-electron subsystem when both electrons recede from the residual proton in opposite directions and equal distances from the nucleus. To include this dynamical screening (and therefore this theory is called DS3C), while still treating all two-body potentials in an exact manner, it is advantageous to separate dynamical from kinematical features of the three-body system and consider the latter properties in an appropriate coordinate system. First, to decouple kinematical from dynamical quantities, for the eigenfunction Ψ of the total Hamiltonian $\mathcal{H}$, at the total energy E, we write

$$\begin{aligned}\Psi(\mathbf{r}_a,\mathbf{r}_b) &= N\Psi^r(\mathbf{r}_a,\mathbf{r}_b)\\ &= N\ \exp(i\mathbf{r}_a\cdot\mathbf{k}_a + i\mathbf{r}_b\cdot\mathbf{k}_b)\overline{\Psi}(\mathbf{r}_a,\mathbf{r}_b),\end{aligned} \tag{1}$$

where $\mathbf{r}_{a/b}$ are the positions of the two electrons with respect to the nucleus, and $\mathbf{k}_{a/b}$ are the momenta conjugate to these coordinates, respectively. The normalization factor N is deduced from the requirement

$$\begin{aligned}|N|^2\ \langle\Psi^r(\mathbf{r}_a,\mathbf{r}_b;\mathbf{k}_a,\mathbf{k}_b)|\Psi^r(\mathbf{r}_a,\mathbf{r}_b;\mathbf{k}'_a,\mathbf{k}'_b)\rangle\\ = \delta^3(\mathbf{k}_a-\mathbf{k}'_a)\,\delta^3(\mathbf{k}_b-\mathbf{k}'_b).\end{aligned} \tag{2}$$

The plane-wave part of Eq. (1) is an eigenfunction of the kinetic-energy operator with eigenvalue E. Thus the modification to the plane-wave motion, which is described by $\overline{\Psi}(\mathbf{r}_{ij},\mathbf{R}_k)$, is due to the presence of the total potential, and can be determined as an eigenfunction of a differential operator H (with zero eigenvalue) [26]. To obtain an insight into the properties of H, the problem is reformulated in the curvilinear coordinate system (only outgoing-wave boundary conditions are considered here)

$$\begin{aligned}\{\xi_k = r_j + \hat{\mathbf{k}}_j\cdot\mathbf{r}_j;\xi_m = r_j\},\quad j\in\{a,b,ab\};k\in[1,3],\\ m\in[4,6],\end{aligned} \tag{3}$$

where $\mathbf{r}_{ab}$ and $\mathbf{k}_{ab}$ are the interelectronic relative coordinate and its conjugate momentum, respectively. The directions of the momenta $\mathbf{k}_j, j\in\{a,b,ab\}$ are denoted by $\hat{\mathbf{k}}_j$. As shown in Ref. [26], the three-body operator H can be decomposed

into two *parametrically* coupled differential operators; an operator $H_{\rm par}$ which is differential in the *parabolic* coordinates $\xi_{1,2,3}$ only, and an operator differential in the rotationally invariant coordinates r_a, r_b, and r_{ab}. An additional mixing term, which is due to the off-diagonal elements of the metric tensor, couples internal to parabolic motion. It is the last term which prevents the separability of the three-body Schrödinger equation. The key point is that the differential operator $H_{\rm par}$ is exactly separable in the coordinates $\xi_{1\ldots3}$, since it factorizes as

$$H_{\rm par}=\sum_{j=1}^{3} H_{\xi_j}, \quad [H_{\xi_j},H_{\xi_i}]=0, \quad \forall\ i,j\in\{1,2,3\}, \quad (4)$$

where, after factoring out the relative plane-wave motion, H_{ξ_j} is the Hamiltonian for two-body Rutherford scattering expressed in parabolic coordinates [37]. Hence, within the approximation $H\approx H_{\rm par}$, the three-body system is considered as the sum of three spatially decoupled two-body Coulomb systems on the two-body energy shell. At a given total energy E, the exact regular eigenfunction of the operator H, within the approximation $H\approx H_{\rm par}$, thus has the explicit form

$$\begin{aligned}\overline{\Psi}_{\rm DS3C}(\xi_{1\ldots6};\mathbf{k}_a,\mathbf{k}_b)&\\ &={}_1F_1(i\beta_a,1,-ik_a\xi_1)\,{}_1F_1(i\beta_b,1,-ik_b\ \ \xi_2)\\ &\quad\times{}_1F_1(i\beta_{ab},1,-ik_{ab}\xi_3). \quad (5)\end{aligned}$$

The eigenstate $\Psi_{\rm DS3C}$ of $\mathcal{H}$ is then readily deduced from Eq. (1). In Eq. (5), ${}_1F_1(a,b,x)$ denotes the confluent hypergeometric function and β_j, $j\in\{a,b,ab\}$ are the Sommerfeld parameters

$$\beta_j=\frac{Z_j}{v_j}, \quad j\in\{a,b,ab\}, \quad (6)$$

with v_j being the velocities corresponding to the momenta $\mathbf{k}_j$ and Z_j, $j\in\{a,b,ab\}$ the electron-nucleus and electron-electron product charges, respectively. The operator H_{ξ_j} depends parametrically on the coordinates $\xi_{4\ldots6}$, e.g., through the two-body Coulomb potential. This parametric dependence of H_{ξ_j} on internal degrees of freedom can be exploited to introduce coupling of each two-body subsystem to the third particle [26] by assuming that an individual two-body Coulomb interaction retains its functional form; i.e., it is of the form $\overline{V_j}=Z_j/r_j, j\in\{a,b,ab\}$. Its strength (expressed through Z_j), however, is determined by all two-body interactions. Considering that this coupling can depend only on internal coordinates (the total potential is rotationally invariant) we end up with $Z_j=Z_j(\xi_{4\ldots6})$. In Ref. [26] the functions $Z_j(\xi_{4\ldots6})$ were given, which preserve the total potential and incorporate the motion along the Wannier ridge [27–36]. To ensure invariance of the Schrödinger equation under the introduction of the product charges $Z_j(\xi_{4\ldots6})$ the condition

$$\sum_j \frac{Z_j(\xi_{4\ldots6})}{r_j}=\frac{-1}{r_a}+\frac{-1}{r_b}+\frac{1}{r_{ab}}, \quad j\in\{a,b,ab\} \quad (7)$$

has to be fulfilled. The constructed wave function $\Psi_{\rm DS3C}$ is compatible with the boundary conditions specified by the shape and size of the triangle formed by the three particles, i.e., it is, to leading order, an asymptotic solution of the three-body Schrödinger equation if the aforementioned triangle tends to a line (two particles are close to each other and far away from the third) or in the case where, for an arbitrary shape, the size of this triangle becomes infinite. The latter limit implies that all interparticle coordinates $r_{a,b,ab}$ must grow with the same order, otherwise we eventually fall back to the limit of the three-particle triangle being reduced to a line [26], as described above. The applicability of the wave function $\Psi_{\rm DS3C}$ to scattering reactions is hampered by the involved functional dependence leading to the complications encountered with the AM method, as discussed in the introduction. Furthermore, the incorporation of the ionization dynamics at shorter distances brings about the intrinsic disadvantage that, in contrast to the 3C approach, the construction of $\Psi_{\rm DS3C}$ has to be individually undertaken for given charge and mass states of the three particles. This is comprehensible since properties of the total potential are inherent to the particular three-body system under investigation. As far as the uniqueness of $\Psi_{\rm DS3C}$ is concerned, it should be mentioned that this function is an approximate solution. Various choices for Z_j result in different parts, $H-H_{\rm par}$, of the total Hamiltonian $\mathcal{H}$ being neglected. The best choice for Z_j would minimize $H-H_{\rm par}$. In the course of constructing $\Psi_{\rm DS3C}$, it has not been possible to show that $H-H_{\rm par}$ is minimal in the entire Hilbert space (minimal only in the asymptotic region and along the Wannier mode). Hence, the part $H-H_{\rm par}$ can be regarded as the ''free parameter'' in this theory. It should be emphasized, however, that there is no physical or mathematical reason to believe that, for example, the 3C wave function, which is a special case of $\Psi_{\rm DS3C}$, is more unique than $\Psi_{\rm DS3C}$, even though the product charges used by the 3C wave function are uniquely given by $Z_a=-1=Z_b$ and $Z_{ab}=1$.

As shown in Ref. [16] the normalization of the 3C wave function can be deduced in the sense of Eq. (2). To my knowledge, this procedure has not been accessible in the cases of $\Psi_{\rm DS3C}$ and AM wave functions. Normalization of $\Psi_{\rm DS3C}$ through flux arguments, in the manner discussed above, resulted in position-dependent normalization [21,38] which is clearly at variance with Eq. (2). To overcome this difficulty (and that associated with the six-dimensional numerical integration) we note that the position dependence of $Z_j(r_a,r_b,r_{ab})$ occurs (due to dimensionality considerations) through ratios of the interparticle distances. Thus this dependence can be converted into velocity dependence by assuming that

$$\frac{r_i}{r_j}\propto\frac{v_i}{v_j}. \quad (8)$$

The proportionality constant in Eq. (8) could be of an arbitrary functional dependence. It should be emphasized that approximation (8) is not a classical one, i.e., it is not assumed that the particles' motions proceed along classical trajectories [conversely, if the motion were classically free, Eq. (8) holds]. It merely means that the total potential is exactly diagonalized in the phase space where Eq. (8) is satisfied, as

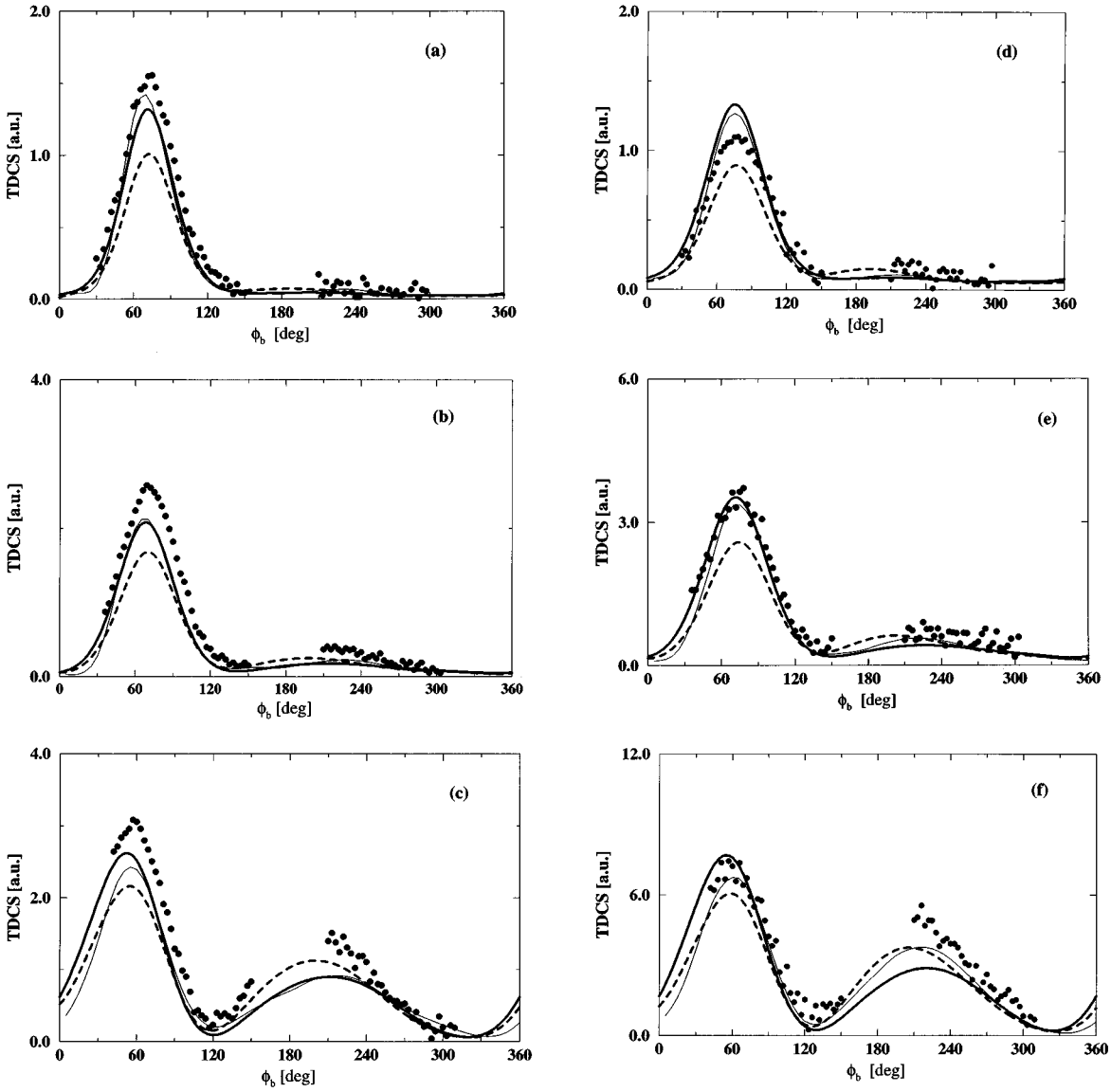

FIG. 1. The triply differential cross section (TDCS) for the coplanar electron-impact ionization of atomic hydrogen. In (a) one electron is detected under a fixed angle of $\phi_a = 344°$ with respect to the incident direction $\mathbf{k}_i$, whereas the other one is detected under the varying angle ϕ_b and with fixed energy $E_b = 10$ eV. The incident energy is $E_i = 150$ eV. Experimental data are from Ref. [4]. The solid thick curve represents the DS3C results, whereas the CCC calculations [13] yield the light solid curve. the dashed curve is the 3C results. In (b) the angle of the fast electron is fixed to $\phi_a = 350°$, in (c) $\phi_a = 356°$, in (d) $E_b = 5$ eV and $\phi_a = 344°$, in (e) $E_b = 5$ eV, and $\phi_a = 350°$, in (f) $E_b = 5$ eV and $\phi_a = 356°$, in (g) $E_b = 3$ eV and $\phi_a = 344°$, in (h) $E_b = 3$ eV and $\phi_a = 350°$ and in (i) $E_b = 3$ eV and $\phi_a = 356°$.

readily deduced from Eq. (7). Equation (8) renders possible the normalization of Ψ_{DS3C} in the sense of Eq. (2), since in this case we obtain $Z_j = Z_j(k_a, k_b, k_{ab})$ and the arguments used in Ref. [16] can be repeated to deduce for N the expression

$$N = \prod_j N_j,$$

$$N_j = \exp[-\beta_j(k_a, k_b, k_{ba})\pi/2]\Gamma[1 - i\beta_j(k_a, k_b, k_{ba})],$$

$$j \in \{a, b, ba\}. \tag{9}$$

An additional advantage of employing approximation (8) is that it allows the incorporation of the Wannier threshold law of double escape [27–36,39]. This results in the velocity-dependent product charges [40]

$$Z_{ba}(\mathbf{v}_a, \mathbf{v}_b) = [1 - (f\ \ g)^2 a^{b_1}] a^{b_2}, \tag{10}$$

$$Z_a(\mathbf{v}_a, \mathbf{v}_b) = -1 + (1 - Z_{ba}) \frac{v_a^{1+a}}{(v_a^a + v_b^a) v_{ab}}, \tag{11}$$

$$Z_b(\mathbf{v}_a, \mathbf{v}_b) = -1 + (1 - Z_{ba}) \frac{v_b^{1+a}}{(v_a^a + v_b^a) v_{ab}}. \tag{12}$$

The functions occurring in Eqs. (10) and (11) are defined as

$$f := \frac{3 + \cos^2 4\alpha}{4}, \quad \tan\alpha = \frac{r_a}{r_b}, \tag{13}$$

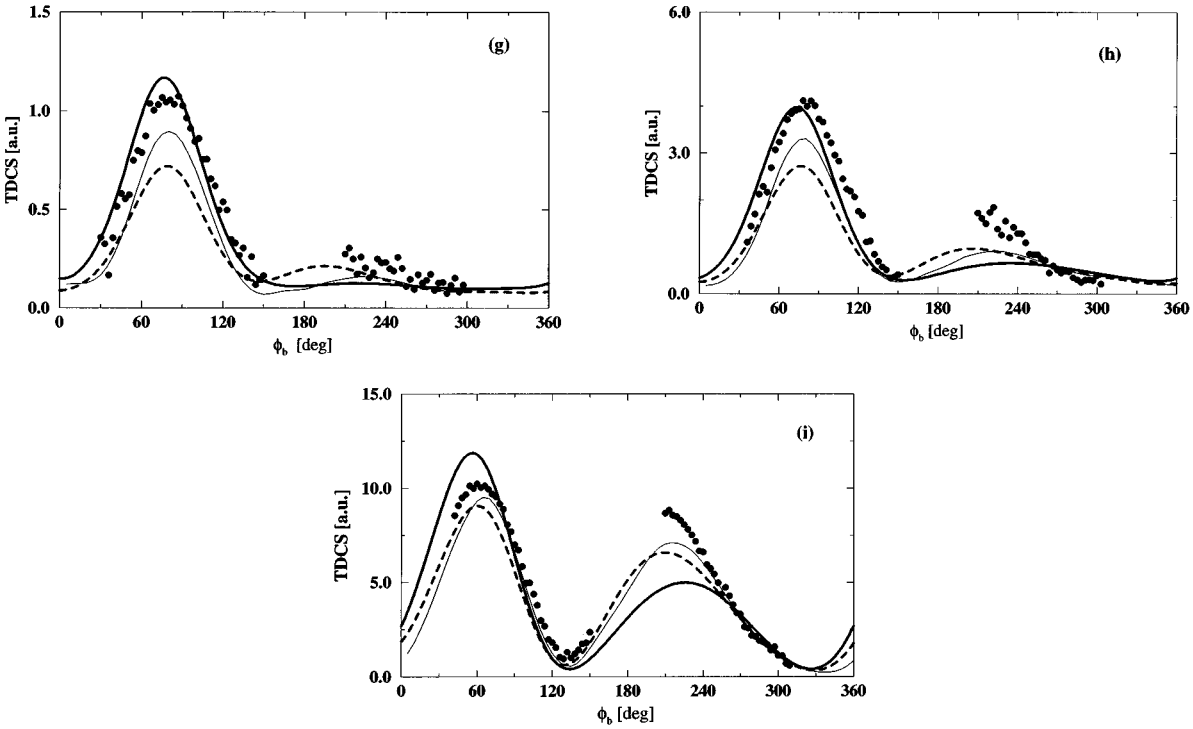

FIG. 1. (*Continued*).

$$g := \frac{v_{ab}}{v_a + v_b}, \tag{14}$$

$$b_1 := \frac{2 v_a v_b \cos\theta_{ab}/2}{v_a^2 + v_b^2}, \tag{15}$$

$$b_2 := g(-0.5 + \mu), \tag{16}$$

$$a := \frac{E}{E + 0.5}, \tag{17}$$

where E is being measured in atomic units and $\mu = 1.127$ is the Wannier index in the case considered here. The interelectronic relative angle θ_{ab} is given by $\theta_{ab} := \cos^{-1}\hat{\mathbf{v}}_a \cdot \hat{\mathbf{v}}_b$. In case of higher excess energies ($E \gg 1$) it is readily verified that $a \to 1$ [Eq. (17)], and all modifications of charges (10)–(12) which are due to incorporating the Wannier threshold law become irrelevant. Charges (10)–(12) then reduce to those given in Ref. [26], with Eq. (8) being applied. From the functional forms of charges (10)–(12) it is clear that when two particles approach each other (in velocity space) they experience their full two-body Coulomb interactions, whereas the third one ''sees'' a net charge equal to the sum of the charges of the two close particles.

The wave function Ψ_{DS3C}, constructed with charges (10)–(12), proved to be quite successful in predicting the absolute and relative angular distributions at quite low energies [5,40–42]. Additionally, the spin-non-resolved total ionization cross section as well as the spin asymmetry are satisfactorily described by this method from threshold up to intermediate energies [26,40]. Here we present a comprehensive comparison with available experimental $(e,2e)$ data from H$(1s)$ in the coplanar asymmetric energy-sharing kinematics at the incident energies $E_i = 250$, 150, and 54.4 eV.

II. ANGULAR DISTRIBUTIONS

For electron-impact ionization of atomic hydrogen, the spin-non-resolved triply differential cross section (TDCS) for the coincident detection of the two continuum electrons is the statistically weighted average of singlet and triplet scattering

$$\sigma_{\mathrm{TDCS}}(\mathbf{k}_a, \mathbf{k}_b) = (2\pi)^4 \frac{k_a\, k_b}{k_i} \left(\tfrac{1}{4}|T^s|^2 + \tfrac{3}{4}|T^t|^2\right), \tag{18}$$

where $\mathbf{k}_i$ is the momentum of the incident projectile. The singlet and triplet transition matrix elements T^s and T^t, respectively, derive from the corresponding transition operators $\mathcal{T}^s$ and $\mathcal{T}^t$, where

$$\mathcal{T}^s = (1 + \mathcal{P}_{ab})\mathcal{T}_{fi}(\mathbf{k}_a, \mathbf{k}_b),$$

$$\mathcal{T}^t = (1 - \mathcal{P}_{ab})\mathcal{T}_{fi}(\mathbf{k}_a, \mathbf{k}_b). \tag{19}$$

The action of the exchange operator $\mathcal{P}_{ab}$ on the $\mathcal{T}_{fi}$ operator is given by $\mathcal{P}_{ab}\mathcal{T}_{fi}(\mathbf{k}_a, \mathbf{k}_b) = \mathcal{T}_{fi}(\mathbf{k}_b, \mathbf{k}_a)$. The prior, position-space representation of $\mathcal{T}_{fi}(\mathbf{k}_a, \mathbf{k}_b)$ is given by

$$T_{fi}(\mathbf{k}_a, \mathbf{k}_b) = \langle \Psi | V_i | \Phi_{\mathbf{k}_i} \rangle. \tag{20}$$

The wave function Ψ is defined by Eq. (1), whereas the three-body system in the initial channel is described by $|\Phi_{\mathbf{k}_i}\rangle$. Assuming $|\Phi_{\mathbf{k}_i}\rangle$ to be the asymptotic initial state, i.e., $\langle \mathbf{r}_a, \mathbf{r}_b | \Phi_{\mathbf{k}_i} \rangle$ is a product of an incoming plane wave representing the incident projectile electron and an undistorted $1s$ state of atomic hydrogen, the perturbation operator V_i

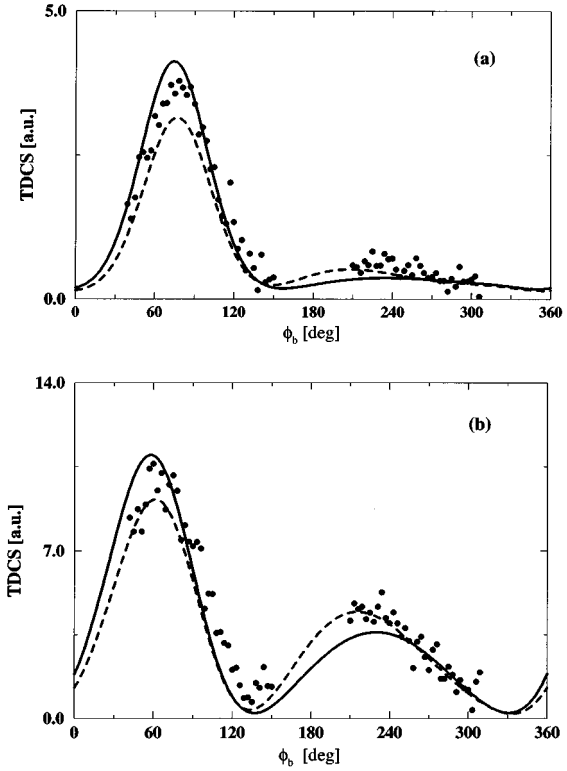

FIG. 2. The same kinematical arrangements as in Fig. 1 but the incident energy is increased to $E_i=250$ eV. In (a) $E_b=5$ eV and $\phi_a=352°$, and in (b) $E_b=5$ eV and $\phi_a=357°$. The curves are the same as in Fig. 1. CCC calculations are not available here.

occurring in Eq. (20) is given by $1/|\mathbf{r}_a-\mathbf{r}_b|-1/r_a$ (which is the part of the total Hamiltonian not diagonalized by $|\Phi_{\mathbf{k}_i}\rangle$). In what follows we choose the x axis as the incident direction $\hat{\mathbf{k}}_i$. The final-state electrons are detected in a coplanar geometry, i.e., $\mathbf{k}_i\cdot(\mathbf{k}_a\times\mathbf{k}_b)=0$. The z axis lies along the direction perpendicular to the scattering plane, i.e., parallel to $\hat{\mathbf{k}}_a\times\hat{\mathbf{k}}_b$. The polar and azimuthal angles of the vector $\mathbf{k}_a$ ($\mathbf{k}_b$) are denoted by θ_a,ϕ_a (θ_b,ϕ_b), respectively. In the coplanar geometry considered here the polar angles are fixed to $\theta_a=\pi/2=\theta_b$. For the sake of clarity, the DS3C calculations with product charges (10)–(12) and within approximation (8) are contrasted only with experiments, and the 3C and CCC results. Comparison of CCC and 3C with 3DWBA and PSCC can be found in Ref. [13], while Ref. [21] compares 3C calculations with the results of the AM model as well as with those of the DS3C, without approximation (8), and with the wave function being normalized by the flux method, as mentioned earlier. In Figs. 1(a)–1(i) the TDCS's for the incident energy of $E_i=150$eV are depicted along with the absolute measurement, as normalized to photoionization cross sections [4]. In general, we note a satisfactory, although not perfect, agreement of the DS3C results with experimental findings. The role of final-state interactions in determining the shape and magnitude of the TDCS has been analyzed in full detail in Refs. [5,41,43,44], and is not repeated here. We remark, however, that the present results confirm the analysis made in Ref. [41] in that three-body coupling primarily affects the magnitude of the TDCS rather than its shape. This is readily concluded by comparing the 3C and DS3C results

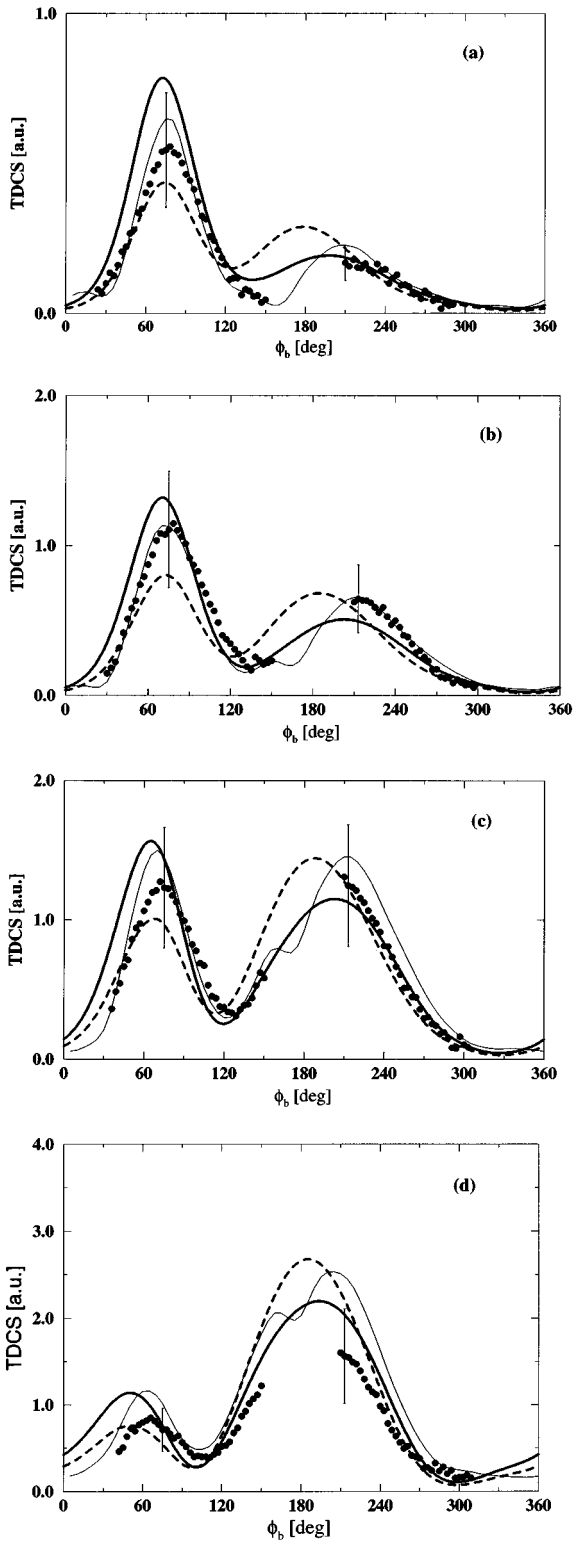

FIG. 3. The same coplanar asymmetric geometry as in Fig. 1; however, the incident energy is decreased to $E_i=54.4$ eV. In (a) $E_b=5$ eV and $\phi_a=337°$, whereas in (b) $E_b=5$ eV and $\phi_a=344°$, in (c) $E_b=5$ eV and $\phi_a=350°$, and, finally, in (d) $E_b=5$ eV and $\phi_a=356°$. Experimental data are taken from Ref. [16]. The error bars indicate the uncertainty in the absolute value of the TDCS [46]. Curves are the same as in Fig. 1.

since, in the former case, three-body coupling is neglected, whereas the merit of the DS3C is the inclusion of this coupling. The general trend is that the 3C model underestimates the magnitude of the TDCS but reproduces, however, the angular shape with sufficient accuracy, as shown in Ref. [15]. The reason for this shortcoming of the 3C model is an incorrect weighting of different scattering amplitudes which alters their interference behavior [5,41]. This underestimation of cross sections by the 3C model persists down to threshold. In fact, as is well known, at lower excess energies the 3C model grossly underestimates the measured absolute value of the cross sections. This behavior, also similar to that observed in Figs. 1(a)–1(i), is not the result of a wrong interference pattern but rather due to a vanishing density of states of the ''unscreened'' electron-electron scattering subsystem.

Generally, differences between the CCC and the DS3C are marginal and, in some cases, both of them are clearly beyond a perfect agreement with the data. In Ref. [13] it is stated that the CCC is ''essentially without approximations.'' Hence, the agreement between the DS3C and the CCC results can lead to the conclusion that the approximations made to arrive at the DS3C wave function are justified in the geometries studied here. In fact, it can be shown analytically that the neglected part H-$H_{\rm par}$ vanishes at higher excess energies [26] [$\lim_{k_j\xi_j\to\infty}(H-H_{\rm par})\to 0$]. Unfortunately, the moderate incident energies and the still remaining differences between experiment and theory shed doubt on this conclusion.

In Ref. [21] calculations were performed using the DS3C without approximation (8). As stated above, the normalization then has to be deduced from the asymptotic flux rather than according to Eq. (2). This procedure yielded a position-dependent normalization [38]. The predicted cross sections turned out to be substantially different from the DS3C results presented here and in some cases substantial discrepancies with experiments were observed. Unfortunately, the ''approximate'' normalization procedure prevents an unambiguous assessment of the approximation $H-H_{\rm par}\approx 0$ which has been made to arrive at the radial part of the wave function. This same argument applies to the TDCS calculations within the AM model.

At higher impact energies [Figs. 2(a) and 2(b)] the 3C and DS3C results converge to each other, whereas in this geometry no CCC calculations are available.

At lower excess energies [Figs. 3(a)–3(d)] differences between various theoretical models extend to the shape of the TDCS. In particular the CCC yields additional subsidiary shoulders in the TDCS. As yet, there is no physical explanation for the appearance of those structures while the two dominant peaks can still be roughly identified as binary and recoil peaks. In fact, at an excess energy as low as 13.6 eV the TDCS still possesses the double-peak structure [5,41]. In this low-energy region it has been shown [5,41] that the 3C fails to reproduce the measured TDCS in shape and magnitude, whereas the DS3C offers reasonable, though not perfect, predictions. As done in Refs. [5,41], the influence of final-state interactions as well as the effects of three-body coupling on the cross sections, shown in Figs. 3(a)-3(d), have been investigated [45]. The conclusions drawn from this study indicate that the origin and the rough positions of the two peaks occurring in Figs. 3(a)–3(d) can be traced to single, and sequential, double-binary collisions. The heights of these peaks is determined by three-body coupling. A study of the spin-resolved TDCS in the geometry corresponding to Figs. 3(a)–3(d) revealed a rich structure of the spin asymmetry $A:=(|T^s|^2-|T^t|^2)/(|T^s|^2+3|T^t|^2)$ [45]. The origin of this variation is basically unexplained as yet. At higher energies and small momentum transfer (Figs. 1 and 2) the TDCS is determined by direct ionization events. Hence the magnitude of the spin asymmetry is vanishingly small.

III. CONCLUSIONS

Contrasting a fully numerical treatment of $(e,2e)$ reactions, such as the CCC approach, with approximate analytical methods, such as 3C and DS3C, yields additional insight into the mathematical and physical structure of the three-body Coulomb problem. Deviations of the results of approximate analytical methods from those predicted by exact numerical approaches can be used as an indicator for the strength of the neglected part of the total Hamiltonian to arrive at these analytical approximations. Unfortunately, the discrepancies between theory and experiments, as observed in Figs. 1 and 3, leave some doubts about the reliability of such a procedure. Hence it is highly desirable to establish some benchmark *absolute* measurements for atomic hydrogen against which various models can be judged. Hydrogenic targets are of particular importance since most $(e,2e)$ theoretical models impose additional approximations in order to deal with $(e,2e)$ processes from many-electron targets.

The DS3C results presented in this work, combined with those at low impact energies and the integrated cross-section results [5,40–42], lead to the conclusion that the part $H-H_{\rm par}$ of $\mathcal{H}$, which has been disregarded to arrive at the DS3C wave function, has minor effects on the measured $(e,2e)$ cross sections in a wide range of the six-dimensional space $\mathbf{k}_a\otimes\mathbf{k}_b$.

ACKNOWLEDGMENTS

I am grateful to Steve Buckman and Erich Weigold for many helpful comments on the manuscript. I also would like to thank Igor Bray and Jochen Röder for communicating their data in tabular form. This work was supported by the Alexander von Humboldt Foundation and the Australian National University.

[1] H. Ehrhardt, M. Schulz, T. Tekaat, and K. Willmann, Phys. Rev. Lett. **22**, 89 (1969).

[2] U. Amaldi, A. Egioli, R. Marconero, and G. Pizella, Rev. Sci. Instrum. **40**, 1001 (1969).

[3] B. Lohmann, I. E. McCarthy, A. T. Stelbovics, and E. Weigold, Phys. Rev. A **30**, 758 (1984).

[4] H. Ehrhardt, K. Jung, G. Knoth, and P. Schlemmer, Z. Phys. D **1**, 3 (1986).

[5] J. Berakdar, J. Röder, J. S. Briggs, and H. Ehrhardt, J. Phys. B **29**, 6203 (1996).
[6] F. W. Byron, Jr. and C. J. Joachain, Phys. Rep. **179**, 211 (1989).
[7] I. E. McCarthy and E. Weigold, Rep. Prog. Phys. **54**, 781 (1991).
[8] J. S. Briggs, Comments At. Mol. Phys. **23**, 155 (1989).
[9] D. H. Madison, R. V. Calhoun, and W. N. Shelton, Phys. Rev. A **16**, 552 (1977).
[10] F. Rouet, R. J. Tweed, and J. Langlois, J. Phys. B **29**, 1767 (1996).
[11] E. P. Curran and H. R. J. Walters, J. Phys. B **20**, 337 (1987).
[12] E. P. Curran, C. T. Whelan, and H. R. J. Walters, J. Phys. B **24**, L19 (1991).
[13] I. Bray, D. A. Konovalov, I. E. McCarthy, and A. T. Stelbovics, Phys. Rev. A **50**, R2818 (1994).
[14] G. Garibotti and J. E. Miraglia, Phys. Rev. A **21**, 572 (1980).
[15] M. Brauner, J. S. Briggs, and H. Klar, J. Phys. B **22**, 2265 (1989).
[16] M. Brauner, J. S. Briggs, H. Klar, J. T. Broad, T. Rösel, K. Jung, and H. Ehrhardt, J. Phys. B **24**, 657 (1991).
[17] J. Berakdar, H. Klar, M. Brauner, and J. S. Briggs, Z. Phys. D **16**, 91 (1990).
[18] H. Klar, Z. Phys. D **16**, 231 (1990).
[19] H. Klar, D. A. Konovalov, and I. E. McCarthy, J. Phys. B **26**, L711 (1993).
[20] S. Jones, D. H. Madison, A. Franz, and P. L. Altick, Phys. Rev. A **48**, R22 (1993).
[21] S. Jones, D. H. Madison, and D. A. Konovalov, Phys. Rev. A **55**, 444 (1997).
[22] E. O. Alt and A. M. Mukhamedzhanov, Phys. Rev. A **47**, 2004 (1993).
[23] A. W. Malcherek, F. Maulbetsch, and J. S. Briggs, J. Phys. B **29**, 4127 (1996).
[24] S. Lucey, J. Rasch, and C. T. Whelan (unpublished).
[25] A. Englens (private communication).
[26] J. Berakdar, Phys. Rev. A **53**, 2314 (1996); **54**, 1480 (1996).
[27] G. Wannier, Phys. Rev. **90**, 817 (1953).
[28] R. K. Peterkop, J. Phys. B **4**, 513 (1971).
[29] A. R. P. Rau, Phys. Rev. A **4**, 207 (1971).
[30] H. Klar and W. Schlecht, J. Phys. B **9**, 1699 (1976).
[31] H. Klar, J. Phys. B **14**, 3255 (1981).
[32] F. H. Read, in *Electron Impact Ionization*, edited by T. D. Märk and G. H. Dunn (Springer, New York, 1984).
[33] A. R. P. Rau, Phys. Rep. **110**, 369 (1984).
[34] J. M. Feagin, J. Phys. B **17**, 2433 (1984).
[35] J-M. Rost, J. Phys. B **28** 3003 (1995).
[36] J. H. Macek and S. Yu. Ovchinnikov, Phys. Rev. Lett. **74**, 4631 (1995).
[37] H. A. Bethe and E. E. Salpeter, *Quantum Mechanics of One- and Two-Electron Atoms* (Springer, Berlin, 1957).
[38] S. Jones and D. H. Madison (private communication).
[39] The wave function Ψ_{DS3C} correctly describes the Wannier mode. Nonetheless, the Wannier threshold law has to be imposed in course of constructing the DS3C theory. This is due to the fact that the DS3C procedure, by neglecting parts of the kinetic energy, aims at exactly diagonalizing the total potential, whereas in Wannier-type treatments the total potential is expanded around the potential saddle, and the kinetic energy is treated in an exact manner.
[40] J. Berakdar, Aust. J. Phys. **49**, 1095 (1996).
[41] J. Berakdar, Phys. Rev. A **55**, 800 (1997).
[42] J. Berakdar and J. S. Briggs, Phys. Rev. Lett. **72**, 3799 (1994); J. Phys. B **27**, 4271 (1994); **29**, 2289 (1996).
[43] J. Berakdar, in *(e,2e) and Related Processes*, Vol. 44 of *NATO Advanced Study Institute, Series C: (e,2e) and Related Processes*, edited by C. T. Whelan, H. R. J. Walters, A. Lahmam-Bennani, and H. Ehrhardt (Kluwer, Dordrect, 1993), p. 131ff.
[44] J. Berakdar and H. Klar, J. Phys. B **26**, 4219 (1993).
[45] J. Berakdar (unpublished).
[46] J. Röder (private communication).